



HAL
open science

A ring-shaped conduit connects the mother cell and forespore during sporulation in *Bacillus subtilis*

Christopher D. A. Rodrigues, Xavier Henry, Emmanuelle Neumann, Vilius Kurauskas, Laure Bellard, Yann Fichou, Paul Schanda, Guy Schoehn, David Z. Rudner, Cécile Morlot

► To cite this version:

Christopher D. A. Rodrigues, Xavier Henry, Emmanuelle Neumann, Vilius Kurauskas, Laure Bellard, et al.. A ring-shaped conduit connects the mother cell and forespore during sporulation in *Bacillus subtilis*. *Proceedings of the National Academy of Sciences of the United States of America*, 2016, 113 (41), pp.11585-11590. 10.1073/pnas.1609604113 . hal-01378398

HAL Id: hal-01378398

<https://hal.univ-grenoble-alpes.fr/hal-01378398>

Submitted on 27 May 2020

HAL is a multi-disciplinary open access archive for the deposit and dissemination of scientific research documents, whether they are published or not. The documents may come from teaching and research institutions in France or abroad, or from public or private research centers.

L'archive ouverte pluridisciplinaire **HAL**, est destinée au dépôt et à la diffusion de documents scientifiques de niveau recherche, publiés ou non, émanant des établissements d'enseignement et de recherche français ou étrangers, des laboratoires publics ou privés.



Distributed under a Creative Commons Attribution - NonCommercial 4.0 International License

A ring-shaped conduit connects the mother cell and forespore during sporulation in *Bacillus subtilis*

Christopher D. A. Rodrigues^{a,1}, Xavier Henry^{b,1,2}, Emmanuelle Neumann^b, Vilius Kurauskas^b, Laure Bellard^b, Yann Fichou^c, Paul Schanda^b, Guy Schoehn^b, David Z. Rudner^{a,3}, and Cecile Morlot^{b,3}

^aDepartment of Microbiology and Immunobiology, Harvard Medical School, Boston MA 02115; ^bInstitut de Biologie Structurale (IBS), Université Grenoble Alpes-Commissariat à l'Energie Atomique et aux Energies Alternatives-CNRS, 38044 Grenoble, France; and ^cInstitute for Physical Chemistry II, Ruhr-Universität Bochum, 44780 Bochum, Germany

Edited by Thomas J. Silhavy, Princeton University, Princeton, NJ, and approved August 26, 2016 (received for review June 14, 2016)

During spore formation in *Bacillus subtilis* a transenvelope complex is assembled across the double membrane that separates the mother cell and forespore. This complex (called the “A–Q complex”) is required to maintain forespore development and is composed of proteins with remote homology to components of type II, III, and IV secretion systems found in Gram-negative bacteria. Here, we show that one of these proteins, SpoIIAG, which has remote homology to ring-forming proteins found in type III secretion systems, assembles into an oligomeric ring in the periplasmic-like space between the two membranes. Three-dimensional reconstruction of images generated by cryo-electron microscopy indicates that the SpoIIAG ring has a cup-and-saucer architecture with a 6-nm central pore. Structural modeling of SpoIIAG generated a 24-member ring with dimensions similar to those of the EM-derived saucer. Point mutations in the predicted oligomeric interface disrupted ring formation in vitro and impaired forespore gene expression and efficient spore formation in vivo. Taken together, our data provide strong support for the model in which the A–Q transenvelope complex contains a conduit that connects the mother cell and forespore. We propose that a set of stacked rings spans the intermembrane space, as has been found for type III secretion systems.

sporulation | SpoIIAG | type III secretion system | EscJ/PrgK/FlfI | SigG

Transport of proteins across the outer membrane of Gram-negative bacteria requires specialized secretion systems (1, 2). These transenvelope complexes span the inner and outer membranes and use ATP hydrolysis in the cytoplasm to power secretion across the outer membrane. Gram-positive bacteria lack an outer member and in most cases lack these specialized secretion systems. Endospore formation in bacteria such as *Bacillus subtilis* provides an unusual and noteworthy example of a Gram-positive, double-membrane envelope. As a result of the phagocytotic process of engulfment, the developing endospore (called the “forespore”) is released into its sister cell (referred to as the “mother cell”), surrounded by an inner membrane derived from the forespore and an outer membrane derived from the mother cell (Fig. 1B) (3). Intriguingly, the mother cell and forespore assemble a multimeric complex spanning these two membranes that bears similarity to specialized secretion systems and is required to maintain forespore development (4–9). It has been proposed that these proteins constitute a hybrid specialized secretion system with a channel connecting mother cell and forespore. Here we provide direct evidence that this complex contains a ring-like conduit in the space between the two membranes.

B. subtilis differentiates into a stress-resistant spore in response to nutrient limitation (3). The first morphological event in this process is the formation of an asymmetrically placed septum generating a small forespore and larger mother cell. Shortly afterwards, the mother cell membranes migrate around the forespore, generating a cell within a cell. Eight mother cell proteins encoded in the *spoIIA* operon (AA, AB, AC, AD, AE, AF, AG, and AH) and one forespore protein, SpoIIQ (Q), are required during and/or shortly after engulfment to maintain forespore development. Cells lacking any of these nine proteins have the same phenotype: The engulfed

forespores fail to grow to their full size and frequently develop membrane invaginations and appear to collapse (7, 10). In addition, these forespores are unable to maintain transcriptional potential including gene expression under the late-acting forespore transcription factor SigG (5, 7).

Previous work indicates that most of the A–Q proteins reside in a multimeric complex that spans the two membranes surrounding the forespore; for simplicity, we refer to this complex as a “transenvelope complex,” although whether it spans the nascent spore coat remains unclear (7). Q produced in the forespore localizes to the inner forespore membrane and is required for the localization of AH in the outer forespore membrane (11, 12). This localization is mediated by direct protein–protein interaction between the extracellular domains of AH and Q in the intermembrane space (Fig. 1B) (11, 12). Furthermore, coimmunoprecipitation experiments have shown that AB, AD, AE, AF, and AG reside in a multimeric membrane complex (7). Finally, AG has been found to localize in the membranes surrounding the forespore (Fig. 1A), and this localization depends on AH and Q (7).

The role of this complex in maintaining forespore development has been informed by the remote homologies (13) of many of the proteins in this complex (4, 6, 7). AA resembles secretion

Significance

Specialized secretion systems transport proteins across the double-membrane cell envelope of Gram-negative bacteria. Gram-positive bacteria possess a single membrane and lack many of these secretion systems. During endospore formation in Gram-positive bacteria such as *Bacillus subtilis*, a double-membrane envelope surrounds the developing spore. A transenvelope complex with similarities to Gram-negative specialized secretion systems spans the two membranes separating mother cell and endospore. This complex is essential for development and has been hypothesized to serve as a channel for molecular transport between the two cells. Here we show that it contains an oligomeric ring with architecture and dimensions similar to those found in type III secretion systems, providing direct evidence for a conduit connecting mother cell and developing spore.

Author contributions: C.D.A.R., D.Z.R., and C.M. designed research; C.D.A.R., X.H., E.N., V.K., L.B., Y.F., P.S., G.S., D.Z.R., and C.M. performed research; C.D.A.R., X.H., E.N., V.K., Y.F., P.S., G.S., D.Z.R., and C.M. analyzed data; and C.D.A.R., E.N., P.S., G.S., D.Z.R., and C.M. wrote the paper.

The authors declare no conflict of interest.

This article is a PNAS Direct Submission.

Data deposition: The cryo-EM 3D reconstruction map of the D1+D2 rings of SpoIIAG from *Bacillus subtilis* has been deposited in the EMDatabank (EMDB ID code [EMD-4072](https://www.ebi.ac.uk/EMDB/EMDB/4072)).

¹C.D.A.R. and X.H. contributed equally to this work.

²Present address: Institut National de la Recherche Agronomique, UMR 1319 MICALIS, 78352 Jouy-en-Josas, France.

³To whom correspondence may be addressed. Email: cecile.morlot@ibs.fr or rudner@hms.harvard.edu.

This article contains supporting information online at www.pnas.org/lookup/suppl/doi:10.1073/pnas.1609604113/-DCSupplemental.

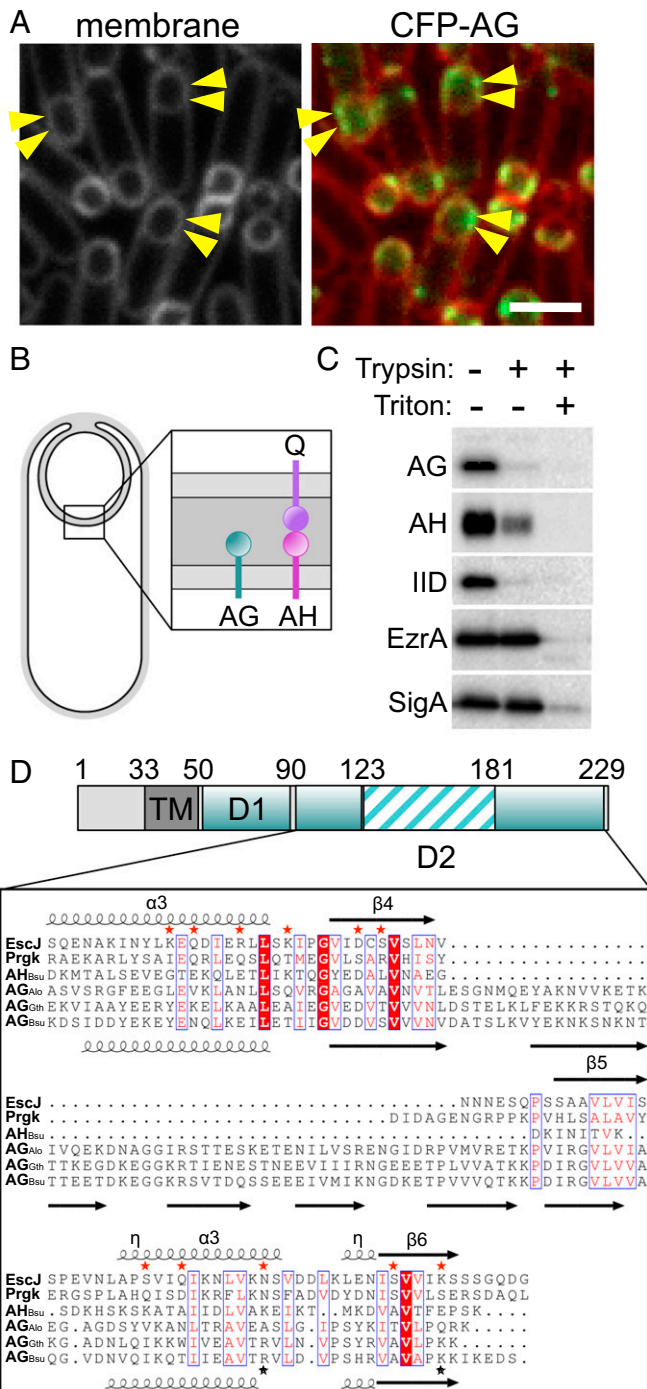


Fig. 1. The extracellular domain of AG has remote homology to PrgK/EscJ proteins in type III secretion systems. (A) CFP-SpoIIAG (CFP-AG, false-colored green) localizes as discrete foci (arrowheads) in the mother cell membranes that surround the forespore. CFP-AG displays weak localization at the second potential polar division site, but the relevance of this localization remains unclear. CFP-AG and membranes (stained with the fluorescent probe TMA-DPH) were visualized by fluorescence microscopy at hour 2 of sporulation. (Scale bar, 2 μ m.) (B) Schematic diagram showing the localization and topology of AG, SpoIIAH (AH), and SpoIIQ (Q) during sporulation. (C) The extracellular domains of AG, AH, and SpoIID (IID) are extracytoplasmic. Immunoblot of a protease susceptibility assay in which sporulating cells were pretoplasted and treated with trypsin with or without Triton X-100. A soluble transcription factor (SigA) and a membrane-anchored cytoplasmic protein (EzrA) were inaccessible to trypsin. (D) Domain structure of AG showing the transmembrane segment (TM) and the extracytoplasmic D1 and D2 domains. Numbering refers to the *B. subtilis* AG sequence.

ATPases found in type IV secretion systems, whereas AB and AE both have domains with remote homology to GspF that helps tether the secretion ATPase to the membrane complex in type II secretion systems. Finally, AF, AG, and AH have remote homology to the EscJ/PrgK family of ring-forming proteins found in type III secretion systems. Importantly, cocrystal structures of a heterodimeric complex consisting of the extracellular domains of AH and Q revealed structural similarity between AH and EscJ/PrgK family members (14, 15). Furthermore, using this structure, the extracellular domains of AH and Q could be modeled into oligomeric rings. Based on the remote sequence homologies and this structural similarity, it has been proposed that AH and Q form a channel in the intermembrane space and that the A-Q complex functions as a specialized secretion system or a feeding tube, allowing the mother cell to nurture the forespore and maintain forespore development (4–7, 14, 15). The structure of this transenvelope complex and whether it functions to transport molecules between the two cells remain important outstanding questions.

Here, we show that the extracellular domains of AG from three endospore formers, *B. subtilis*, *Geobacillus thermodenitrificans*, and *Acetonea longum*, assemble into large oligomeric rings in vitro. 3D reconstruction of images generated by cryo-EM indicates that the *B. subtilis* AG ring has a “cup-and-saucer” architecture, similar to that of the EscJ/PrgK family member FliF, which is part of the flagellar basal body (16). Structural modeling of AG generated a ring with dimensions similar to those of the saucer, and point mutants in the predicted oligomeric interface disrupted ring formation in vitro and impaired SigG activity and spore formation in vivo. These data indicate that the A-Q complex contains a conduit that connects the mother cell and the forespore and support a model in which stacked rings similar to those found in type III secretion systems span the intermembrane space.

Results

The Extracellular Domain of AG Has Remote Homology to the EscJ/PrgK Family. The AG protein has a single N-terminal transmembrane segment and a large soluble domain (Fig. 1D). A sequence alignment of more than 20 AG orthologs using ClustalW (17) indicates that the soluble domain displays low sequence conservation over the first ~40 amino acids (designated “D1”) and higher sequence conservation over the remaining ~140 C-terminal residues (called “D2”) (Fig. 1D). The D2 domain of AG has been reported previously to have remote homology to the EscJ/PrgK family of ring-forming proteins in type III secretion systems (6, 7). Alignment of the D2 domain from AG orthologs with EscJ from *Escherichia coli* EPEC (18) and PrgK from *Salmonella typhimurium* SPI-1 (19, 20) revealed that AG proteins contain two regions (residues 90–123 and 181–229) that share weak sequence and secondary structure similarities with these ring-forming proteins. However, AG orthologs contain an insertion between these regions (residues 124–180) with no homology to known structures (Fig. 1D). This extended D2 domain was recently reported by Bergeron (21). To investigate whether the soluble portion of AG (D1+D2) resides in the cytoplasm or, like AH, in the space between the mother cell and forespore membranes (Fig. 1B), we analyzed its localization by protease susceptibility. Sporulating cells were treated with lysozyme in hypertonic buffer to generate

The sequences of AG from *B. subtilis* (AG^{Bsu}), *G. thermodenitrificans* NG-80 (AG^{Gth}), and *A. longum* (AG^{Ala}) were aligned with *S. typhimurium* SPI-1 and PrgK and *E. coli* EPEC LEE EscJ. Conserved residues are in red boxes; similar residues are shown by red letters boxed in blue. The secondary structures of EscJ and the ones predicted for AG^{Bsu} are indicated above and below the sequence alignment, respectively. Arrows indicate β -strands; α , α -helix; η , 3_{10} -helices. Residues at the oligomeric interface of EscJ protomers are indicated by red stars. Predicted AG^{Bsu} interface residues important for ring formation and sporulation are indicated by with black stars.

protoplasts. The protoplasts then were treated with trypsin followed by immunoblot analysis using anti-AG antibodies. Consistent with the idea that the D1 and D2 domains of AG are extracellular, these domains and the extracellular domain of AH and the sporulation protein SpoIID were susceptible to protease digestion (Fig. 1C). By contrast, an integral membrane protein with a large cytoplasmic domain (EzrA) and a soluble transcription factor (SigA) were both fully protected.

The Extracellular Domain of AG Forms Large Oligomeric Rings. As a first step toward structural determination, we expressed the extracellular domain (D1+D2) of AG from *B. subtilis* (AG_{Bsu}) in *E. coli* and purified it to homogeneity (Fig. 2A). Size-exclusion chromatography resolved the purified protein into two distinct species, a small one eluting at ~ 15 mL and a larger one eluting at ~ 8.5 mL, indicative of an oligomeric complex (Fig. 2A). Calibration using protein standards indicate apparent molecular masses of 22.5 and 550 kDa for the small and large species, respectively. Negative-stain EM of the large molecular weight species revealed homogeneous rings with a large central cavity (Fig. 2C). The majority of the particles had the same orientation and dimensions, with a diameter of ~ 20 nm and an apparent central pore of ~ 7 nm. To investigate whether these structures were unique to *B. subtilis* AG, we expressed and purified the D2 domains from two other AG orthologs (Fig. 2B). One was from *G. thermodenitrificans* (AG_{Gth} , 46% identity to AG_{Bsu}), and the other was from the Gram-negative bacterium *A. longum* (AG_{Alo} , 25% identity to AG_{Bsu}), which differentiates into an endospore. Negative-stain EM revealed ring-shaped structures similar to those of AG_{Bsu} (Fig. 2D). Thus, the ability to assemble into oligomeric rings in vitro is a property shared among distantly related AG family members, suggesting that these rings are a physiologically relevant structure.

To characterize the AG_{Bsu} rings further, we performed analytical ultracentrifugation. Differential sedimentation coefficient distributions $[c(s)]$ (Fig. S1) defined a species at a sedimentation coefficient (S) of 1.5 consistent with an elongated AG_{Bsu} monomer of 19.7 kDa. A second species was determined at 14.5 S, compatible with a 24-mer with a slightly anisotropic shape (frictional ratio $f/f_{min} = 1.5$) and a hydrodynamic radius (R_H) of 7.6 nm. Because analytical ultracentrifugation is accurate to approximately $\pm 10\%$, we tentatively conclude that the AG_{Bsu} ring is composed of 24 protomers. This order of rotational symmetry is similar to that of the EscJ, PrgK, and FliF rings (24 for EscJ/PrgK and 24–26 for FliF) (16, 18, 20), further supporting the idea that members of the SpoIIIA complex resemble the periplasmic rings found in type III secretion systems.

Cryo-EM 3D Reconstruction of the AG_{Bsu} Ring Reveals a Cup-and-Saucer Architecture. More than 15,000 particle images were collected from vitrified samples, and $\sim 6,000$ were analyzed by projection matching (Fig. S2; see *SI Materials and Methods* for details). To obtain a 3D reconstruction, 24-fold rotational symmetry was imposed based on the results from analytical ultracentrifugation. Unfortunately, very few (< 200) side views of the AG_{Bsu} ring were collected (Fig. S2B and D). Accordingly, the resolution of the resulting map (Fig. 2E) was estimated to be ~ 35 Å. Nevertheless, the reconstruction of the AG_{Bsu} ring revealed a cup-and-saucer architecture with a central pore (Fig. 2E). The outer diameter of the saucer was 21 nm, and the outer and inner diameters of the cup were 11 nm and 6 nm, respectively. The height of the cup and saucer together was 8 nm. The AG saucer had dimensions similar to those of the rings formed by PrgK, EscJ, and FliF (outer diameters of 18.7, 18, and 24 nm, respectively) (16, 18, 20). Interestingly, the AG cup is reminiscent of domain R in the FliF ring (16), which forms a cup-like structure that is thought to contact the cylindrical rod of the flagellum that traverses the outer membrane (*Discussion*).

In Silico Modeling of the AG_{Bsu} Monomer and Ring. Despite intensive efforts to provide atomic resolution of the AG ring, we were unable

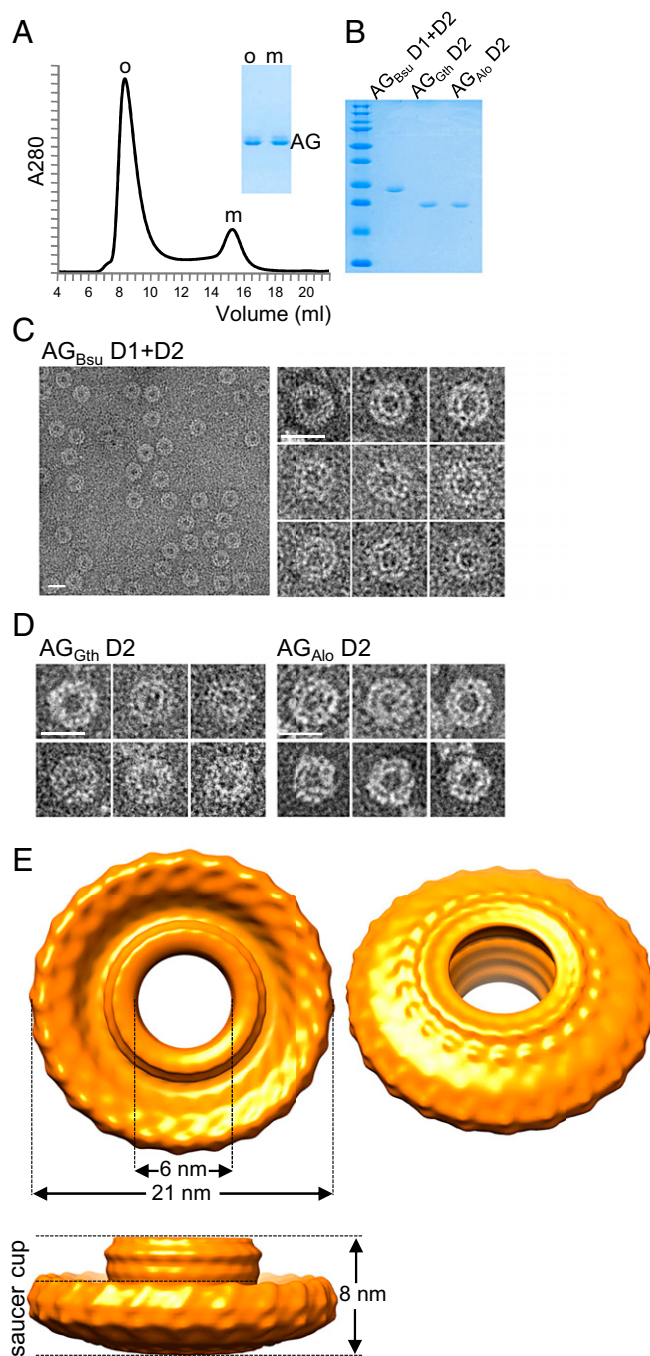


Fig. 2. The extracellular domain of AG forms large oligomeric rings in vitro. (A) Size-exclusion chromatography of the purified AG_{Bsu} D1+D2 protein. The elution volume (from a Superdex 200 column) is plotted on the x axis, and the 280-nm absorbance is plotted on the y axis. The void volume was 7.5 mL. Coomassie-stained gel of the oligomeric (o) and the monomeric (m) fractions is shown. (B) Coomassie-stained gel of the purified D1+D2 protein from *B. subtilis* and the D2 domain from *G. thermodenitrificans* and *A. longum*. (C and D) Negative-stained EM images of AG oligomers purified by size exclusion. (Scale bars, 20 nm.) (E) 3D cryo-EM reconstruction of AG D1+D2 from *B. subtilis*. The models are visualized at 2.0σ .

to obtain crystals that diffracted to high resolution from either the D2 or the D1+D2 domains from AG_{Bsu} , AG_{Gth} , or AG_{Alo} . Accordingly, we performed in silico modeling on the D2 domain of AG_{Bsu} and fitted the structural model into our EM density map. Using the Swiss Model server (22), a model based on the structure of PrgK was generated (Fig. 3A). In the two regions of AG_{Bsu}

homologous to the EscJ/PrgK family (residues 90–123 and 181–229), the model contained high-confidence factors (mean value \pm SD, 0.6 ± 0.2). Modeling of the insertion between these regions (residues 124–180) was more problematic: Confidence factors were particularly low in the regions encompassing residues 124–128 and 155–180 (0.13 ± 0.1) (Fig. S3). However, the region encompassing residues 129–154 was predicted to form a two-stranded antiparallel β -sheet with a mean confidence factor of 0.54 ± 0.2 (Fig. 3A). This latter prediction is supported by in silico secondary structure predictions and the high proportion of β -structures in the AG_{Bsu} rings detected by solid-state NMR (Fig. S4).

Using the regions of the AG_{Bsu} monomer that had structural predictions with confidence factors >0.2 (Fig. S3), we modeled the ring. The domain corresponding to the two regions homologous to EscJ/PrgK (residues 90–123 and 181–224) was placed in the EM map manually, and a 24-fold rotational symmetry was applied. This step was followed by energy minimization using NAMD (23). The resulting 24-member ring could be fit easily into the saucer derived from the EM map with an outer diameter of the ring of 20.9 nm (Fig. 3B and C). However, density at the bottom of the saucer and the entire cup were missing. Because the cup is present in the rings from the D2 domains of AG_{Gth} and AG_{Ala} (Fig. 2D), we suspect that the D1 domain (residues 51–90) from AG_{Bsu}, which was not used in the modeling, does not make up the cup but instead is the missing density in the saucer. In support of this idea, the ring model predicts that the N terminus of the D2 domain is oriented toward the bottom of the saucer. To investigate whether the insertion region in the D2 domain that was predicted to form a two-stranded antiparallel β -sheet (residues 129–154) could be the cup, we independently placed it in the EM map, applied a 24-fold rotational symmetry, and performed energy minimization (23). The resulting β -barrel had inner and outer diameters of 7.4 and 10.4 nm, respectively, that fit

easily into the EM map of the cup (Fig. 3B and C). Although this structural prediction is consistent with our EM 3D reconstruction, residues 124–128 and 155–180 of the insertion region that could not be modeled with high-confidence factors were not included in modeling the ring. We therefore tentatively conclude that the D2 domain constitutes both the cup and saucer observed by EM.

In Vivo Test of the AG Ring Model. To test the ring model, we focused on the oligomeric interface in the two regions homologous to EscJ/PrgK that make up the saucer. The model predicts hydrophilic interactions between Q201, R217, and K223 on one protomer interface and R209, D212, and E106, respectively, on the other (Fig. 4A). We generated site-directed mutations (R209E, R209A, K223E, and K223A) in the D1+D2 expression construct and purified the four mutant proteins. Size-exclusion chromatography revealed that all four had an increase in monomeric species (Fig. 4B and Fig. S5). Analysis of the larger species by negative-stain EM indicates that most contained aggregates or fibers rather than rings (Fig. S5). These data are consistent with R209 and K223 playing a role in oligomerization. To investigate whether oligomerization is important in vivo, we generated R209E and K223E substitutions in the context of the full-length AG gene and tested them for their ability to support SigG activity and efficient sporulation. These mutants were chosen because they were the most monomeric in vitro and produced the least amount of aggregated protein (Fig. 4B and Fig. S5). Sporulating cells harboring AG(R209E) were impaired in SigG activity, had a small forespore phenotype, and were significantly reduced in sporulation efficiency (Fig. 4D). Cells harboring AG(K223E) were also reduced in sporulation efficiency, although not as strongly (approximately fivefold). Importantly, a subset of forespores was smaller and had impaired SigG activity. Both proteins were produced at levels similar to the wild-type control (Fig. 4C). Collectively, these data are consistent with the idea that AG forms a ring in vivo and that this ring is important for the proper function of the A–Q complex in maintaining forespore physiology, SigG activity, and efficient spore formation.

AG Is a Core Component of the A–Q Transenvelope Complex. Previous work suggested that Q and AH represent the core components of a channel that connects the mother cell and forespore (4). Our data indicating that the extracellular domain of AG resides in the intermembrane space and assembles into an oligomeric ring that is important for forespore development suggest that AG is a central part of an A–Q conduit. Accordingly, we returned to the experiments that defined AH and Q as core elements. In previous work, a small in-frame deletion in *pbpG* encoding a class A penicillin-binding protein was found to bypass partially the requirement for most of the components of the A–Q complex for SigG activity (4). The mechanism by which this mutant bypassed the need for members of the complex was (and remains) unclear, but it was used as an assay to perform epistasis tests. Only AH and Q mutants could not be bypassed by the in-frame deletion, suggesting that they constitute the core components. The strains used in these studies were specifically engineered to eliminate the contribution of SigG autoregulation and any role of the negative regulator CsfB (also called “Gin”) on SigG activity. Using these same strains and fluorescence microscopy to monitor SigG activity and forespore development in single cells, we found that a deletion of the entire *spoIII*A operon (including AH) was partially bypassed by the *pbpG* mutation (Fig. S6), indicating that the bypass is independent of the A–Q complex. Furthermore, analysis of SigG activity in strains that retain SigG autoregulation and CsfB revealed that the *pbpG* mutation similarly bypassed AH and AG mutants as well as the operon deletion (Fig. S7). In addition, the small and collapsed forespore phenotypes associated with AH and AG mutants were not suppressed by the *pbpG* mutation (Fig. S8). These results argue that the partial bypass mediated by the PbpG mutant is not a good predictor of core components and, taken together with the data

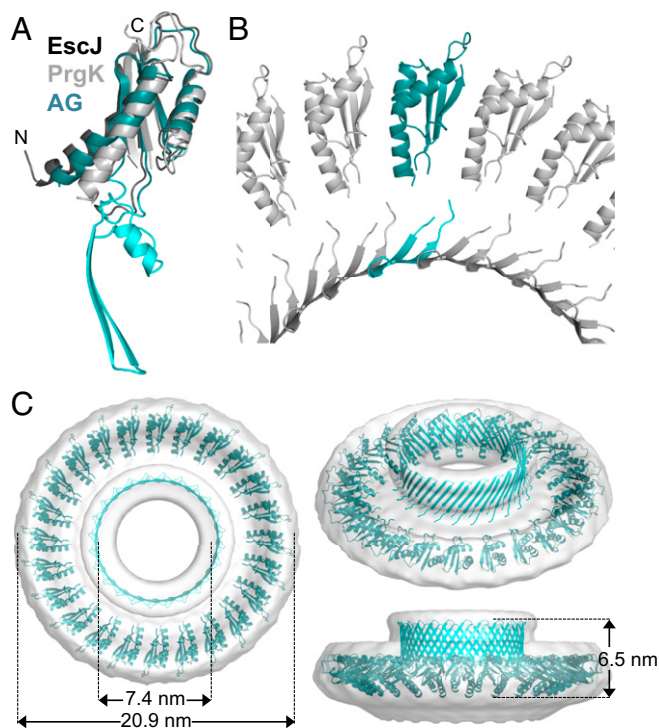


Fig. 3. 3D modeling of the AG ring. (A) Ribbon representation of the raw AG_{Bsu} D2 model (AG) superimposed on the D2 structures of EscJ (dark gray) and PrgK (light gray). The AG_{Bsu} regions homologous to EscJ/PrgK are in teal, and the insertion region is in cyan. (B) Close-up view of the modeled AG_{Bsu} D2 ring. (C) Ribbon representation of the AG_{Bsu} D2 ring model in the EM map density (SI Materials and Methods).

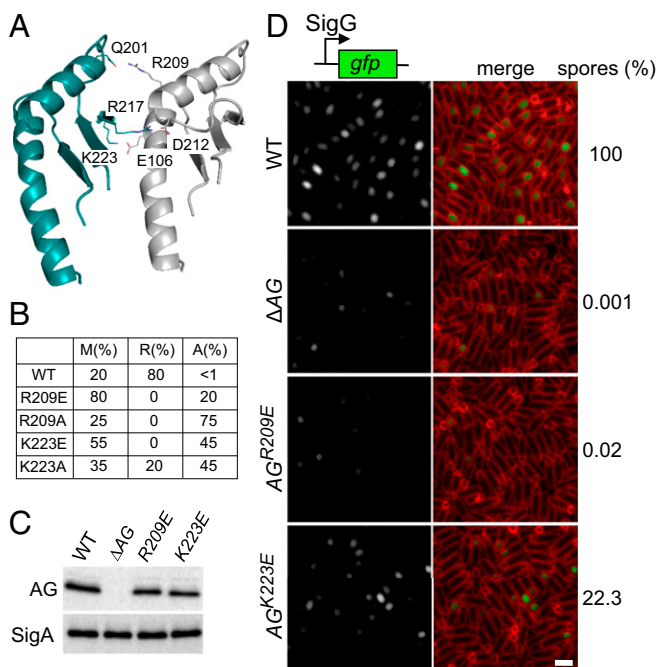


Fig. 4. In vitro and in vivo test of the AG ring model. (A) Close-up view of the interface between two adjacent subunits in the saucer region of the AG_{Bsu} D2 ring model. Residues predicted to make up the oligomeric interface are labeled. (B) Table showing the proportion of monomers (M), rings (R), and aggregates (A) assessed by gel filtration and negative-stain EM for the AG_{Bsu} D1+D2 variants. The primary data can be found in Fig. S5. (C) Immunoblot analysis of whole-cell lysates from sporulating wild-type (BCR1434), Δ AG mutant (BCR776), AG(R209E) (BCR1435), and AG(K223E) (BCR1436) with anti-AG antibodies. SigA levels were monitored to control for loading. (D) SigG activity (Left) and sporulation efficiency (Right) of *B. subtilis* cells with AG mutants. Wild-type (BCR1438), Δ AG mutant (BCR1437), and cells expressing AG(R209E) (BCR1439) or AG(K223E) (BCR1440) were visualized 4 h after the initiation of sporulation. All strains harbor a SigG-responsive promoter (P_{sspB}) fused to GFP. Images of P_{sspB} -GFP fluorescence (Left) and of P_{sspB} -GFP fluorescence images merged with TMA-DPH-stained membranes (Right) are shown. The images were scaled identically. (Scale bar, 2 μ m.)

presented above, suggest that AG and AH both contribute to the conduit that connects the mother cell and the forespore.

Discussion

Here, we have shown that AG homologs from *B. subtilis* and two distantly related species that form endospores assemble into large rings with a cup-and-saucer architecture. Mutations in predicted interface residues in the AG_{Bsu} ring result in impaired ring assembly in vitro and reduced SigG activity and sporulation in vivo. Collectively, these results provide evidence for a conduit between the mother cell and forespore and support the idea that the A–Q complex could function as a channel or secretion complex.

Our modeling suggests that the AG cup results from the oligomerization of a region inserted within the ring-building motif (RBM) that is predicted to contain two long antiparallel β -strands. Intriguingly, the third RBM of FliF in the flagellar basal body also has an insertion region predicted to be rich in β secondary structures (21). Accordingly, we hypothesize that the FliF cup (called the “R region”) may be similarly composed of this insertion and form a large β -barrel. In the case of FliF, the cup faces the outer membrane where it engages the flagellar rod complex (16, 24). Although the orientation of the AG cup is not known, we favor a model in which it also faces toward the forespore (away from the mother cell membrane), because our data suggest that the D1 domain is part of the base of the saucer and this domain is directly preceded by AG’s transmembrane segment (Fig. 1B). In addition, this orientation of the ring is similar to that of the PrgK and EscJ rings in type III secretion systems (18, 20).

The structural similarities between the extracellular domain of AH and EscJ/PrgK proteins and in silico modeling suggested that AH together with Q oligomerize into a pair of rings (14, 15). Our finding that three distinct AG homologs assemble into rings strengthens and extends this model. Because Q is synthesized in the forespore and AH in the mother cell, the Q ring likely resides in close apposition to the forespore membrane followed by AH (Fig. 5). We have previously shown that the localization of AG to the membranes surrounding the forespore requires AH and Q, suggesting that the AG ring could stack against AH by analogy to the stacked rings found in type III secretion systems (2, 18). If, as our data suggest, the AG cup faces toward the forespore, then in the context of this model the cup region would contact the AH ring (Fig. 5). How it does so is unknown at present. To accommodate steric clashes between AH protomers (and, separately, Q protomers), AH–Q ring models containing 12, 15, and 18 subunits have been proposed (14, 15). A 15-member AH–Q ring has a pore size of \sim 7 nm and could not accommodate the AG cup with an outer diameter of \sim 11 nm. Accordingly, in this model, the “lip” of the cup would contact the AH ring. If instead the cup is inserted into the pore of the AH ring, then the latter ring must contain at least 18 protomers. An alternative possibility is that AH assembles into a 24-member ring, which would allow 1:1 interactions between AG and AH subunits, as is the case with PrgK and PrgH (20). It is noteworthy that, in addition to the mother cell-specific (SigE) promoter upstream of the *spoIIIA* operon, there is a second SigE-responsive promoter within the *spoIIIAF* (*AF*) gene (25). This promoter results in increased expression of AG and AH, suggesting that the stoichiometry of these two components is higher than that of the other SpoIIIA proteins in the complex and is consistent with a stacked ring model. Our attempts to generate heteromeric complexes with purified extracellular domains of AG, AH, and Q have been unsuccessful thus far (*SI Materials and Methods*). Addressing the precise stoichiometry and organization of the rings in the A–Q complex will ultimately require a high-resolution structure of the intact complex, ideally purified directly from sporulating cells.

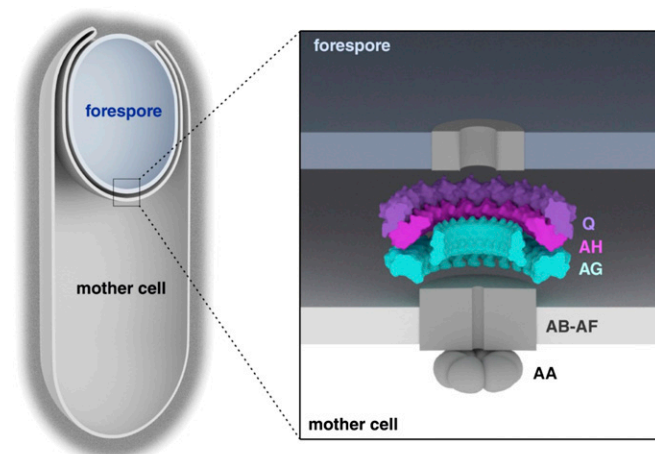


Fig. 5. AG, AH, and Q form stacked rings in the intermembrane space. Schematic diagram showing the A–Q complex in the two membranes that surround the forespore. AH (in magenta) and Q (in purple) are shown as a double ring containing 18 protomers of each, as proposed by Meisner et al. (15). The AG D2 ring model fitted in the experimental EM map is shown in cyan. The other membrane proteins encoded in the *spoIIIA* operon (AB–AF) are shown schematically as a single complex (gray) with a predicted membrane pore. AA is shown as a hexamer by analogy to other secretion ATPases. Evidence suggests the existence of a pore in the forespore membrane (6) (shown schematically in gray); the identity of this protein is unknown.

Extending the analogy between the A–Q complex and type III secretion systems and the flagellar basal body, a needle or inner rod complex might be expected to reside in the pore generated by AG and AH. No proteins currently known to be required for SigG activity are similar to those that make up these tube-like structures. Accordingly, whether such a structure exists in the A–Q complex remains an outstanding question. The absence of any candidate protein for an inner rod or needle raises the possibility that the A–Q complex uses its type III-like proteins to generate a channel (4, 5). In line with this idea, AH, AG, and AF are the only proteins in the A–Q complex that share sequence similarity with proteins found in type III secretion systems. Indeed, AA most closely resembles secretion ATPases found in type IV secretion systems, and the polytopic membrane proteins AB and AE both have domains with remote homology to GspF from type II secretion systems. One popular model that accounts for the absence of an inner rod or needle is that the complex functions as a feeding tube (5) in which the ATPase component and associated integral membrane proteins act as a gate or energy source for transport of undefined molecules across the outer forespore membrane and into the AG/AH/Q channel.

Interestingly, recent work in the endospore former *Clostridium difficile* suggests that the A–Q complex may be dispensable for late forespore gene expression under SigG control and therefore may not play a direct role in maintaining transcriptional potential in the *C. difficile* forespore (8, 9). Intriguingly, both studies identified morphological defects in spore differentiation in the absence of the A–Q complex, suggesting that the complex could play a structural role in maintaining forespore development. These findings raise the possibility that this highly conserved transenvelope complex might not be a secretion complex or a feeding tube. One possibility that is compatible with the remote homologies and structural similarities described here is that the complex is a noncanonical piliation system

and, for example, functions to adhere the two membranes together. In its absence, the forespore develops morphological defects, fails to mature, and, in the case of *B. subtilis*, loses transcriptional potential. Although currently there is no candidate pilin or pseudopilin protein that would connect the two cells, it is possible that, as in the case of the SpoIIIA proteins, this factor has remote or even undetectable homology to counterparts in canonical piliation and type II secretion systems. Future genetic and biochemical studies will be required to distinguish among these models, while structure characterization will help unravel the global architecture of the A–Q complex.

Materials and Methods

All *B. subtilis* strains were derived from the prototrophic strain PY79 (26). Sporulation assays and fluorescence microscopy were performed as previously described (7). All recombinant proteins were overexpressed in *E. coli* Rosetta (DE3) pLysS and were affinity purified as His-SUMO fusions (27) followed by size-exclusion chromatography. For cryo-EM, purified AG_{Bsu} was loaded onto a Quantifoil R2/1 holey grid and vitrified using a Mark IV Vitrobot; images were acquired on a Polara electron microscope. Detailed protocols are provided in *SI Materials and Methods*, and strains, plasmids, and oligonucleotide primers are listed in [Table S1](#).

ACKNOWLEDGMENTS. We thank members of the Vernet, D.Z.R., Dessen, and Bernhardt laboratories for advice and encouragement; Janet Iwasa for figure preparation; Daphna Fenel for negative-stain EM imaging; Amy Camp for sharing strains; and Christine Ebel and Aline Le Roy for analytical ultracentrifugation analyses. Support for this work came from NIH Grant GM086466 (to D.Z.R.) and Agence Nationale de la Recherche (ANR) Grant ANR-11-BSV8-005-01 PILIPATH. This work used the platforms of the Grenoble Instruct Centre (Integrated Structural Biology Grenoble, UMS 3518 CNRS-Commissariat à l’Energie Atomique et aux Energies Alternatives-Université Grenoble Alpes-EMBL), with support from the French Infrastructure for Integrated Structural Biology Initiative (FRISBI) Grant ANR-10-INSB-05-02 and the Grenoble Alliance for Integrated Structural Cell Biology (GRAL) Grant ANR-10-LABX-49-01 within the Grenoble Partnership for Structural Biology (PSB).

- Costa TR, et al. (2015) Secretion systems in Gram-negative bacteria: Structural and mechanistic insights. *Nat Rev Microbiol* 13(6):343–359.
- Burkinshaw BJ, Strynadka NC (2014) Assembly and structure of the T3SS. *Biochim Biophys Acta* 1843(8):1649–1663.
- Tan IS, Ramamurthi KS (2014) Spore formation in *Bacillus subtilis*. *Environ Microbiol Rep* 6(3):212–225.
- Camp AH, Losick R (2008) A novel pathway of intercellular signalling in *Bacillus subtilis* involves a protein with similarity to a component of type III secretion channels. *Mol Microbiol* 69(2):402–417.
- Camp AH, Losick R (2009) A feeding tube model for activation of a cell-specific transcription factor during sporulation in *Bacillus subtilis*. *Genes Dev* 23(8):1014–1024.
- Meisner J, Wang X, Serrano M, Henriques AO, Moran CP, Jr (2008) A channel connecting the mother cell and forespore during bacterial endospore formation. *Proc Natl Acad Sci USA* 105(39):15100–15105.
- Doan T, et al. (2009) Novel secretion apparatus maintains spore integrity and developmental gene expression in *Bacillus subtilis*. *PLoS Genet* 5(7):e1000566.
- Fimlaid KA, Jensen O, Donnelly ML, Siegrist MS, Shen A (2015) Regulation of *Clostridium difficile* spore formation by the SpoIIQ and SpoIIA proteins. *PLoS Genet* 11(10):e1005562.
- Serrano M, et al. (2016) The SpoIIQ-SpoIIAH complex of *Clostridium difficile* controls forespore engulfment and late stages of gene expression and spore morphogenesis. *Mol Microbiol* 100(1):204–228.
- Rodrigues CD, Marquis KA, Meisner J, Rudner DZ (2013) Peptidoglycan hydrolysis is required for assembly and activity of the transenvelope secretion complex during sporulation in *Bacillus subtilis*. *Mol Microbiol* 89(6):1039–1052.
- Blaylock B, Jiang X, Rubio A, Moran CP, Jr, Pogliano K (2004) Zipper-like interaction between proteins in adjacent daughter cells mediates protein localization. *Genes Dev* 18(23):2916–2928.
- Doan T, Marquis KA, Rudner DZ (2005) Subcellular localization of a sporulation membrane protein is achieved through a network of interactions along and across the septum. *Mol Microbiol* 55(6):1767–1781.
- Södberg J, Biegert A, Lupas AN (2005) The HHpred interactive server for protein homology detection and structure prediction. *Nucleic Acids Res* 33(Web Server issue):W244–8.
- Levdikov VM, et al. (2012) Structure of components of an intercellular channel complex in sporulating *Bacillus subtilis*. *Proc Natl Acad Sci USA* 109(14):5441–5445.
- Meisner J, Maehigashi T, André I, Dunham CM, Moran CP, Jr (2012) Structure of the basal components of a bacterial transporter. *Proc Natl Acad Sci USA* 109(14):5446–5451.
- Suzuki H, Yonekura K, Namba K (2004) Structure of the rotor of the bacterial flagellar motor revealed by electron cryomicroscopy and single-particle image analysis. *J Mol Biol* 337(1):105–113.
- Combet C, Blanchet C, Geourjon C, Deléage G (2000) NPS@: Network protein sequence analysis. *Trends Biochem Sci* 25(3):147–150.
- Yip CK, et al. (2005) Structural characterization of the molecular platform for type III secretion system assembly. *Nature* 435(7042):702–707.
- Bergeron JR, et al. (2015) The modular structure of the inner-membrane ring component PrgK facilitates assembly of the type III secretion system basal body. *Structure* 23(1):161–172.
- Schraiddt O, Marlovits TC (2011) Three-dimensional model of Salmonella’s needle complex at subnanometer resolution. *Science* 331(6021):1192–1195.
- Bergeron JR (2016) Structural modeling of the flagellum MS ring protein Flif reveals similarities to the type III secretion system and sporulation complex. *PeerJ* 4:e1718.
- Bordoli L, et al. (2009) Protein structure homology modeling using SWISS-MODEL workspace. *Nat Protoc* 4(1):1–13.
- Phillips JC, et al. (2005) Scalable molecular dynamics with NAMD. *J Comput Chem* 26(16):1781–1802.
- Thomas DR, Francis NR, Xu C, DeRosier DJ (2006) The three-dimensional structure of the flagellar rotor from a clockwise-locked mutant of *Salmonella enterica* serovar Typhimurium. *J Bacteriol* 188(20):7039–7048.
- Guillot C, Moran CP, Jr (2007) Essential internal promoter in the spoIIIA locus of *Bacillus subtilis*. *J Bacteriol* 189(20):7181–7189.
- Youngman PJ, Perkins JB, Losick R (1983) Genetic transposition and insertional mutagenesis in *Bacillus subtilis* with *Streptococcus faecalis* transposon Tn917. *Proc Natl Acad Sci USA* 80(8):2305–2309.
- Uehara T, Parzych KR, Dinh T, Bernhardt TG (2010) Daughter cell separation is controlled by cytotkinetic ring-activated cell wall hydrolysis. *EMBO J* 29(8):1412–1422.
- Harwood CR, Cutting SM (1990) *Molecular Biological Methods for Bacillus* (Wiley, Hoboken, NJ).
- Schaeffer P, Millet J, Aubert JP (1965) Catabolic repression of bacterial sporulation. *Proc Natl Acad Sci USA* 54(3):704–711.
- Broder DH, Pogliano K (2006) Forespore engulfment mediated by a ratchet-like mechanism. *Cell* 126(5):917–928.
- Mindell JA, Grigorieff N (2003) Accurate determination of local defocus and specimen tilt in electron microscopy. *J Struct Biol* 142(3):334–347.
- Ludtke SJ, Baldwin PR, Chiu W (1999) EMAN: Semiautomated software for high-resolution single-particle reconstructions. *J Struct Biol* 128(1):82–97.
- Frank J, et al. (1996) SPIDER and WEB: Processing and visualization of images in 3D electron microscopy and related fields. *J Struct Biol* 116(1):190–199.
- van Heel M, Schatz M (2005) Fourier shell correlation threshold criteria. *J Struct Biol* 151(3):250–262.
- Scheres SH (2012) RELION: Implementation of a Bayesian approach to cryo-EM structure determination. *J Struct Biol* 180(3):519–530.
- Wriggers W (2012) Conventions and workflows for using Situs. *Acta Crystallogr D Biol Crystallogr* 68(Pt 4):344–351.
- Goddard TD, Huang CC, Ferrin TE (2007) Visualizing density maps with UCSF Chimera. *J Struct Biol* 157(1):281–287.